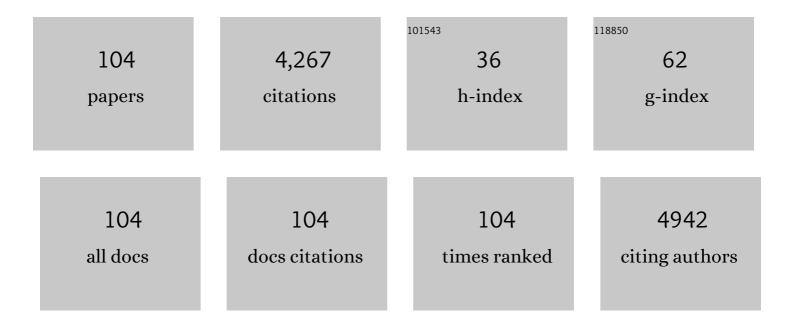
List of Publications by Year in descending order

Source: https://exaly.com/author-pdf/5225368/publications.pdf Version: 2024-02-01



KUN-MULEE

#	Article	IF	CITATIONS
1	High-performance perovskite solar cells based on dopant-free hole-transporting material fabricated by a thermal-assisted blade-coating method with efficiency exceeding 21%. Chemical Engineering Journal, 2022, 427, 131609.	12.7	37
2	High Efficiency Quasiâ€⊋D/3D Pb–Ba Perovskite Solar Cells via Phenethylammonium Chloride Addition. Solar Rrl, 2022, 6, .	5.8	4
3	Effect of Thiophene Insertion on X-Shaped Anthracene-Based Hole-Transporting Materials in Perovskite Solar Cells. Polymers, 2022, 14, 1580.	4.5	2
4	Pd-Free synthesis of dithienothiophene-based oligoaryls for effective hole-transporting materials by optimized Cu-catalyzed annulation and direct C–H arylation. Organic Chemistry Frontiers, 2022, 9, 2821-2829.	4.5	5
5	Efficient perovskite solar cells with low J-V hysteretic behavior based on mesoporous Sn-doped TiO2 electron extraction layer. Chemical Engineering Journal, 2022, 445, 136761.	12.7	15
6	Enhanced efficiency and stability of quasi-2D/3D perovskite solar cells by thermal assisted blade coating method. Chemical Engineering Journal, 2021, 405, 126992.	12.7	20
7	A star-shaped cyclopentadithiophene-based dopant-free hole-transport material for high-performance perovskite solar cells. Chemical Communications, 2021, 57, 6444-6447.	4.1	16
8	Step-saving synthesis of star-shaped hole-transporting materials with carbazole or phenothiazine cores <i>via</i> optimized C–H/C–Br coupling reactions. RSC Advances, 2021, 11, 8879-8885.	3.6	7
9	Unveiling the surface precipitation effect of Ag ions in Ag-doped TiO2 nanofibers synthesized by one-step hydrothermal method for photocatalytic hydrogen production. Journal of the Taiwan Institute of Chemical Engineers, 2021, 120, 291-299.	5.3	13
10	Molecularly Engineered Cyclopenta[2,1- <i>b</i> ;3,4- <i>b</i> ′]dithiophene-Based Hole-Transporting Materials for High-Performance Perovskite Solar Cells with Efficiency over 19%. ACS Applied Energy Materials, 2021, 4, 4719-4728.	5.1	21
11	Development of Stepâ€Saving Alternative Synthetic Pathways for Functional Ï€â€Conjugated Materials. Chemical Record, 2021, , .	5.8	6
12	Reducing Defects in Organic-Lead Halide Perovskite Film by Delayed Thermal Annealing Combined with KI/I2 for Efficient Perovskite Solar Cells. Nanomaterials, 2021, 11, 1607.	4.1	6
13	Highâ€Performance Stable Perovskite Solar Cell via Defect Passivation With Constructing Tunable Graphitic Carbon Nitride. Solar Rrl, 2021, 5, 2100257.	5.8	9
14	Highâ€Performance Stable Perovskite Solar Cell via Defect Passivation With Constructing Tunable Graphitic Carbon Nitride. Solar Rrl, 2021, 5, 2170084.	5.8	2
15	Solid-state reaction process for high-quality organometallic halide perovskite thin film. Solar Energy Materials and Solar Cells, 2021, 227, 111014.	6.2	3
16	Organic Solvent Resistant Nanocomposite Films Made from Selfâ€precipitated Ag/TiO 2 Nanofibers and Cellulose Nanofiber for Harmful Volatile Organic Compounds Photodegradation. Advanced Materials Interfaces, 2021, 8, 2101467.	3.7	5
17	Organic Solvent Resistant Nanocomposite Films Made from Selfâ€precipitated Ag/TiO ₂ Nanofibers and Cellulose Nanofiber for Harmful Volatile Organic Compounds Photodegradation (Adv. Mater. Interfaces 22/2021). Advanced Materials Interfaces, 2021, 8, 2170129.	3.7	0
18	Microstructure and Biological Properties of Electrospun In Situ Polymerization of Polycaprolactone-Graft-Polyacrylic Acid Nanofibers and Its Composite Nanofiber Dressings. Polymers, 2021, 13, 4246.	4.5	10

#	Article	IF	CITATIONS
19	Control of TiO2 electron transport layer properties to enhance perovskite photovoltaics performance and stability. Organic Electronics, 2020, 77, 105406.	2.6	24
20	Antimicrobial Activity of Electrospun Polyvinyl Alcohol Nanofibers Filled with Poly[2-(tert-butylaminoethyl) Methacrylate]-Grafted Graphene Oxide Nanosheets. Polymers, 2020, 12, 1449.	4.5	19
21	Thiophene-Fused Butterfly-Shaped Polycyclic Arenes with a Diphenanthro[9,10- <i>b</i> :9′,10′- <i>d</i>]thiophene Core for Highly Efficient and Stable Perovskite Solar Cells. ACS Applied Materials & Interfaces, 2020, 12, 50495-50504.	8.0	11
22	Achieving Highâ€Performance Perovskite Photovoltaic by Morphology Engineering of Lowâ€Temperature Processed Znâ€Doped TiO 2 Electron Transport Layer. Small, 2020, 16, 2002201.	10.0	13
23	Boosting the power conversion efficiency of perovskite solar cells based on Sn doped TiO2 electron extraction layer via modification the TiO2 phase junction. Solar Energy, 2020, 205, 390-398.	6.1	13
24	Thermal assisted blade coating methylammonium lead iodide films with non-toxic solvent precursors for efficient perovskite solar cells and sub-module. Solar Energy, 2020, 204, 337-345.	6.1	14
25	Controlling the Morphology and Interface of the Perovskite Layer for Scalable High-Efficiency Solar Cells Fabricated Using Green Solvents and Blade Coating in an Ambient Environment. ACS Applied Materials & Interfaces, 2020, 12, 26041-26049.	8.0	41
26	Polymer Additives for Morphology Control in Highâ€Performance Leadâ€Reduced Perovskite Solar Cells. Solar Rrl, 2020, 4, 2070063.	5.8	4
27	Polymer Additives for Morphology Control in Highâ€Performance Leadâ€Reduced Perovskite Solar Cells. Solar Rrl, 2020, 4, 2000093.	5.8	15
28	Barium doping effect on the photovoltaic performance and stability of MA0.4FA0.6BaxPb1-xlyCl3-y perovskite solar cells. Applied Surface Science, 2020, 521, 146451.	6.1	7
29	Study of electrospun polyacrylonitrile fibers with porous and ultrafine nanofibril structures: Effect of stabilization treatment on the resulting carbonized structure. Journal of Applied Polymer Science, 2019, 136, 48218.	2.6	8
30	Step-efficient access to new starburst hole-transport materials with carbazole end-groups for perovskite solar cells <i>via</i> direct C–H/C–Br coupling reactions. Materials Chemistry Frontiers, 2019, 3, 2041-2045.	5.9	11
31	Spiro-tBuBED: a new derivative of a spirobifluorene-based hole-transporting material for efficient perovskite solar cells. Journal of Materials Chemistry A, 2019, 7, 5934-5937.	10.3	14
32	Making benzotrithiophene derivatives dopant-free for perovskite solar cells: Step-saving installation of π-spacers by a direct C–H arylation strategy. Journal of Materials Chemistry A, 2019, 7, 24765-24770.	10.3	22
33	Effect of anti-solvent mixture on the performance of perovskite solar cells and suppression hysteresis behavior. Organic Electronics, 2019, 65, 266-274.	2.6	18
34	Rational Design of Cyclopenta[2,1â€b;3,4â€b′]dithiopheneâ€bridged Hole Transporting Materials for Highly Efficient and Stable Perovskite Solar Cells. Energy Technology, 2019, 7, 307-316.	3.8	18
35	Direct Câ^'H Arylation Meets Perovskite Solar Cells: Tinâ€Free Synthesis Shortcut to Highâ€Performance Holeâ€Transporting Materials. Chemistry - an Asian Journal, 2018, 13, 1510-1515.	3.3	21
36	One-pot synthesis of D–π–D–π–D type hole-transporting materials for perovskite solar cells by sequential C–H (hetero)arylations. Chemical Communications, 2018, 54, 11495-11498.	4.1	15

#	Article	IF	CITATIONS
37	Highly efficient and stable semi-transparent perovskite solar modules with a trilayer anode electrode. Nanoscale, 2018, 10, 17699-17704.	5.6	34
38	Enhancing the efficiency of perovskite solar cells using mesoscopic zinc-doped TiO ₂ as the electron extraction layer through band alignment. Journal of Materials Chemistry A, 2018, 6, 16920-16931.	10.3	71
39	Sequential Preparation of Dual‣ayer Fluorineâ€Doped Tin Oxide Films for Highly Efficient Perovskite Solar Cells. ChemSusChem, 2018, 11, 3234-3242.	6.8	7
40	Improved Solar-Driven Photocatalytic Performance of Highly Crystalline Hydrogenated TiO2 Nanofibers with Core-Shell Structure. Scientific Reports, 2017, 7, 40896.	3.3	41
41	Cross-Dehydrogenative Coupling (CDC) as Key-Transformations to Various Dâʾ'π–A Organic Dyes: C–H/C–H Synthetic Study Directed toward Dye-Sensitized Solar Cells Applications. Journal of Organic Chemistry, 2017, 82, 3538-3551.	3.2	15
42	Thickness effects of thermally evaporated C60 thin films on regular-type CH3NH3PbI3 based solar cells. Solar Energy Materials and Solar Cells, 2017, 164, 13-18.	6.2	32
43	Sn―and Pdâ€Free Synthesis of D–ï€â€"A Organic Sensitizers for Dyeâ€Sensitized Solar Cells by Cuâ€Catalyzed Direct Arylation. ChemSusChem, 2017, 10, 2284-2290.	6.8	13
44	Performance Characterization of Dye-Sensitized Photovoltaics under Indoor Lighting. Journal of Physical Chemistry Letters, 2017, 8, 1824-1830.	4.6	51
45	Controlled Deposition and Performance Optimization of Perovskite Solar Cells Using Ultrasonic Spray oating of Photoactive Layers. ChemSusChem, 2017, 10, 1405-1412.	6.8	62
46	International round-robin inter-comparison of dye-sensitized and crystalline silicon solar cells. Journal of Power Sources, 2017, 340, 309-318.	7.8	9
47	Selection of anti-solvent and optimization of dropping volume for the preparation of large area sub-module perovskite solar cells. Solar Energy Materials and Solar Cells, 2017, 172, 368-375.	6.2	59
48	Enhancing perovskite solar cell performance and stability by doping barium in methylammonium lead halide. Journal of Materials Chemistry A, 2017, 5, 18044-18052.	10.3	88
49	Endâ€Capping Groups for Smallâ€Molecule Organic Semiconducting Materials: Synthetic Investigation and Photovoltaic Applications through Direct C–H (Hetero)arylation. European Journal of Organic Chemistry, 2017, 2017, 111-123.	2.4	11
50	The Effect of Post-Baking Temperature and Thickness of ZnO Electron Transport Layers for Efficient Planar Heterojunction Organometal-Trihalide Perovskite Solar Cells. Coatings, 2017, 7, 215.	2.6	6
51	Enhanced open-circuit voltage of dye-sensitized solar cells using Bi-doped TiO2 nanofibers as working electrode and scattering layer. Solar Energy, 2016, 135, 22-28.	6.1	21
52	Holeâ€Transporting Materials Based on Twisted Bimesitylenes for Stable Perovskite Solar Cells with High Efficiency. ChemSusChem, 2016, 9, 274-279.	6.8	48
53	DPP containing D–ï€â€"A organic dyes toward highly efficient dye-sensitized solar cells. Dyes and Pigments, 2016, 125, 27-35.	3.7	25
54	Connecting Direct Câ^'H Arylation Reactions with Dye‧ensitized Solar Cells: A Shortcut to D–A–π–A Organic Dyes. ChemSusChem, 2015, 8, 3222-3227.	6.8	17

#	Article	IF	CITATIONS
55	Thickness effects of ZnO thin film on the performance of tri-iodide perovskite absorber based photovoltaics. Solar Energy, 2015, 120, 117-122.	6.1	43
56	Unraveling the high performance of tri-iodide perovskite absorber based photovoltaics with a non-polar solvent washing treatment. Solar Energy Materials and Solar Cells, 2015, 141, 309-314.	6.2	72
57	The cause for the low efficiency of dye sensitized solar cells with a combination of ruthenium dyes and cobalt redox. Physical Chemistry Chemical Physics, 2015, 17, 10170-10175.	2.8	24
58	Raman and photoluminescence investigation of CdS/CdSe quantum dots on TiO2 nanoparticles with multi-walled carbon nanotubes and their application in solar cells. Vibrational Spectroscopy, 2015, 80, 66-69.	2.2	10
59	Preparation of High Transmittance Platinum Counter Electrode at an Ambient Temperature for Flexible Dye-Sensitized Solar Cells. Electrochimica Acta, 2014, 135, 578-584.	5.2	25
60	Fabrication of high transmittance and low sheet resistance dual ion doped tin oxide films and their application in dye-sensitized solar cells. Thin Solid Films, 2014, 570, 7-15.	1.8	12
61	Titanium dioxide coated on titanium/stainless steel foil as photoanode for high efficiency flexible dye-sensitized solar cells. Journal of Power Sources, 2014, 269, 789-794.	7.8	17
62	Monoanchoring (Dâ€Dâ€Ï€â€A) and Dianchoring (Dâ€Dâ€(Ï€â€A) ₂) Organic Dyes Featuring Triaryla Donors Composed of Fluorene and Carbazole. Asian Journal of Organic Chemistry, 2014, 3, 886-898.	mine 2.7	8
63	Syntheses of size-varied nanorods TiO2 and blending effects on efficiency for dye-sensitized solar cells. Journal of Power Sources, 2013, 235, 297-302.	7.8	9
64	Enhanced efficiency of bifacial and back-illuminated Ti foil based flexible dye-sensitized solar cells by decoration of mesoporous SiO2 layer on TiO2 anode. Journal of Power Sources, 2013, 232, 1-6.	7.8	14
65	Efficient and stable back-illuminated sub-module dye-sensitized solar cells by decorating SiO2 porous layer with TiO2 electrode. RSC Advances, 2013, 3, 9994.	3.6	16
66	Surface passivation: The effects of CDCA co-adsorbent and dye bath solvent on the durability of dye-sensitized solar cells. Solar Energy Materials and Solar Cells, 2013, 108, 70-77.	6.2	33
67	Degradation Analysis of Thermal Aged Back-Illuminated Dye-Sensitized Solar Cells. Journal of the Electrochemical Society, 2012, 159, B430-B433.	2.9	10
68	Ionic liquid diffusion properties in tetrapod-like ZnO photoanode for dye-sensitized solar cells. Journal of Power Sources, 2012, 216, 330-336.	7.8	13
69	High-efficiency cascade CdS/CdSe quantum dot-sensitized solar cells based on hierarchical tetrapod-like ZnO nanoparticles. Physical Chemistry Chemical Physics, 2012, 14, 13539.	2.8	46
70	High contrast all-solid-state electrochromic device with 2,2,6,6-tetramethyl-1-piperidinyloxy (TEMPO), heptyl viologen, and succinonitrile. Solar Energy Materials and Solar Cells, 2012, 99, 135-140.	6.2	37
71	Improved performance of flexible dye-sensitized solar cells by introducing an interfacial layer on Ti substrates. Journal of Materials Chemistry, 2011, 21, 5114.	6.7	57
72	Improvement on the long-term stability of flexible plastic dye-sensitized solar cells. Journal of Power Sources, 2011, 196, 8897-8903.	7.8	35

#	Article	IF	CITATIONS
73	Co-sensitization promoted light harvesting for plastic dye-sensitized solar cells. Journal of Power Sources, 2011, 196, 2416-2421.	7.8	64
74	High efficiency flexible dye-sensitized solar cells by multiple electrophoretic depositions. Journal of Power Sources, 2011, 196, 3683-3687.	7.8	70
75	The influence of tetrapod-like ZnO morphology and electrolytes on energy conversion efficiency of dye-sensitized solar cells. Electrochimica Acta, 2010, 55, 8422-8429.	5.2	37
76	A dye-sensitized photo-supercapacitor based on PProDOT-Et2 thick films. Journal of Power Sources, 2010, 195, 6232-6238.	7.8	89
77	Plastic dye-sensitized photo-supercapacitor using electrophoretic deposition and compression methods. Journal of Power Sources, 2010, 195, 6225-6231.	7.8	130
78	Effects of mesoscopic poly(3,4-ethylenedioxythiophene) films as counter electrodes for dye-sensitized solar cells. Thin Solid Films, 2010, 518, 1716-1721.	1.8	80
79	Carbazole Containing Ruâ€based Photoâ€sensitizer for Dyeâ€sensitized Solar Cell. Journal of the Chinese Chemical Society, 2010, 57, 1127-1130.	1.4	8
80	A High Contrast Hybrid Electrochromic Device Containing PEDOT, Heptyl Viologen, and Radical Provider TEMPO. Journal of the Electrochemical Society, 2010, 157, P75.	2.9	19
81	Heteroleptic ruthenium antenna-dye for high-voltage dye-sensitized solar cells. Journal of Materials Chemistry, 2010, 20, 7158.	6.7	50
82	Incorporation of a stable radical 2,2,6,6-tetramethyl-1-piperidinyloxy (TEMPO) in an electrochromic device. Solar Energy Materials and Solar Cells, 2009, 93, 2102-2107.	6.2	10
83	All-solid-state electrochromic device based on poly(butyl viologen), Prussian blue, and succinonitrile. Solar Energy Materials and Solar Cells, 2009, 93, 1755-1760.	6.2	55
84	Binary room-temperature ionic liquids based electrolytes solidified with SiO2 nanoparticles for dye-sensitized solar cells. Journal of Power Sources, 2009, 190, 573-577.	7.8	48
85	On the addition of conducting ceramic nanoparticles in solvent-free ionic liquid electrolyte for dye-sensitized solar cells. Solar Energy Materials and Solar Cells, 2009, 93, 1411-1416.	6.2	39
86	Dye-sensitized solar cells with a micro-porous TiO2 electrode and gel polymer electrolytes prepared by in situ cross-link reaction. Solar Energy Materials and Solar Cells, 2009, 93, 2003-2007.	6.2	39
87	High performance dye-sensitized solar cells containing 1-methyl-3-propyl imidazolinium iodide-effect of additives and solvents. Journal of Electroanalytical Chemistry, 2009, 633, 146-152.	3.8	34
88	High efficiency quasi-solid-state dye-sensitized solar cell based on polyvinyidene fluoride-co-hexafluoro propylene containing propylene carbonate and acetonitrile as plasticizers. Journal of Photochemistry and Photobiology A: Chemistry, 2009, 207, 224-230.	3.9	39
89	A high-performance counter electrode based on poly(3,4-alkylenedioxythiophene) for dye-sensitized solar cells. Journal of Power Sources, 2009, 188, 313-318.	7.8	172
90	Influences of different TiO2 morphologies and solvents on the photovoltaic performance of dye-sensitized solar cells. Journal of Power Sources, 2009, 188, 635-641.	7.8	107

#	Article	IF	CITATIONS
91	Enhancing the performance of dye-sensitized solar cells based on an organic dye by incorporating TiO2 nanotube in a TiO2 nanoparticle film. Electrochimica Acta, 2009, 54, 4123-4130.	5.2	44
92	Efficient and stable plastic dye-sensitized solar cells based on a high light-harvesting ruthenium sensitizer. Journal of Materials Chemistry, 2009, 19, 5009.	6.7	72
93	Highly porous PProDOT-Et2 film as counter electrode for plastic dye-sensitized solar cells. Physical Chemistry Chemical Physics, 2009, 11, 3375.	2.8	100
94	A novel photoelectrochromic device with dual application based on poly(3,4-alkylenedioxythiophene) thin film and an organic dye. Journal of Power Sources, 2008, 185, 1505-1508.	7.8	56
95	A photo-physical and electrochemical impedance spectroscopy study on the quasi-solid state dye-sensitized solar cells based on poly(vinylidene fluoride-co-hexafluoropropylene). Journal of Power Sources, 2008, 185, 1605-1612.	7.8	56
96	Incorporating carbon nanotube in a low-temperature fabrication process for dye-sensitized TiO2 solar cellsâ~†. Solar Energy Materials and Solar Cells, 2008, 92, 1628-1633.	6.2	203
97	EIS analysis on low temperature fabrication of TiO2 porous films for dye-sensitized solar cells. Electrochimica Acta, 2008, 53, 7514-7522.	5.2	226
98	2,3-Disubstituted Thiophene-Based Organic Dyes for Solar Cells. Chemistry of Materials, 2008, 20, 1830-1840.	6.7	401
99	A study on the electron transport properties of TiO2 electrodes in dye-sensitized solar cells. Solar Energy Materials and Solar Cells, 2007, 91, 1416-1420.	6.2	111
100	A comparative study of gel polymer electrolytes based on PVDF-HFP and liquid electrolytes, containing imidazolinium ionic liquids of different carbon chain lengths in DSSCs. Solar Energy Materials and Solar Cells, 2007, 91, 1467-1471.	6.2	33
101	Effects of co-adsorbate and additive on the performance of dye-sensitized solar cells: A photophysical study. Solar Energy Materials and Solar Cells, 2007, 91, 1426-1431.	6.2	72
102	On the use of triethylamine hydroiodide as a supporting electrolyte in dye-sensitized solar cells. Solar Energy Materials and Solar Cells, 2007, 91, 1432-1437.	6.2	12
103	The effects of hydrothermal temperature and thickness of TiO2 film on the performance of a dye-sensitized solar cell. Solar Energy Materials and Solar Cells, 2006, 90, 2391-2397.	6.2	153
104	The influence of surface morphology of TiO2 coating on the performance of dye-sensitized solar cells. Solar Energy Materials and Solar Cells, 2006, 90, 2398-2404.	6.2	78